DOI: 10.37190/abb/207865

Estimating Dynamic Plantar Pressure Distribution from Wearable Inertial Sensors Using a Hybrid CNN-BiLSTM Architecture

Yihan Qian[1], Dong Sun[1], Zifan Xia[1], Enze Shao[1,2], Yang Song[3], József Sárosi[4], István Bíró[2,4], Zixiang Gao[5], Yaodong Gu[1*]

[1]Faculty of Sports Science, Ningbo University, Ningbo, China
[2]Doctoral School on Safety and Security Sciences, Óbuda University, Budapest, Hungary
[3]Department of Biomedical Engineering, Faculty of Engineering, The Hong Kong Polytechnic University, Hong Kong, China
[4]Faculty of Engineering, University of Szeged, Szeged, Hungary
[5]Human Performance Laboratory, Faculty of Kinesiology, University of Calgary, Calgary, Canada
[*]Corresponding author: Yaodong Gu, Faculty of Sports Science, Ningbo University, Ningbo, China, e-mail address: guyaodong@hotmail.com

Submitted: 3rd June 2025
Accepted: 3rd July 2025

Abstract

Purpose: Plantar pressure distribution is a crucial indicator in gait analysis, with significant value in clinical diagnoses and sports optimization. Traditional measurement methods, however, are often limited by expensive equipment and laboratory settings. This study aimed to develop an accurate, portable, and cost-effective method using a deep learning model based on data from wearable Inertial Measurement Units (IMU) to predict comprehensive plantar pressure distributions. Methods: We propose a hybrid model combining a Convolutional Neural Network (CNN) and a Bidirectional Long Short-Term Memory (BiLSTM) network. The CNN extracts local features from IMU data; the BiLSTM captures temporal dependencies; a temporal attention mechanism optimizes the prediction of key time steps; and body weight information is integrated to accommodate individual differences. Results: Experimental results show that in 10-fold cross-validation, the model achieves a Mean Squared Error of 0.98 and a Structural Similarity Index of 0.89, demonstrating excellent prediction accuracy and distribution similarity. Conclusions: This study provides a cost-effective method for plantar pressure analysis, which is expected to be integrated into wearable devices for real-time gait monitoring, with applications in rehabilitation and sports optimization.

Keywords: IMU; Plantar pressure; CNN; LSTM; attention mechanism

1 Introduction

The analysis of plantar pressure distribution plays an important role in both clinical practice and applied research settings. For example, these pressure data can be used to assess human motion function[7], monitor foot pathologies[4], and improve footwear design to optimize athletic performance[28]-[30]. However, traditional methods for measuring plantar pressure, such as insole-based pressure measure systems, are typically expensive, lack portability, and are restricted to laboratory environments, thereby limiting their broader application in practical settings.

In recent years, with the development of wearable sensor technology, inertial measurement units (IMUs) have gained widespread attention due to their portability, low cost, and ease of use[14],[22]. IMUs can capture lower limb kinematic parameters such as segment accelerations, angular velocities, and joint angles in real-time, providing a new approach for gait analysis[16].

Hamdi et al. concluded that IMUs can accurately capture most of the key biomechanical variables that describe human gait. As long as the system can effectively describe normal walking gait, it can also be used for capturing other gait activities, such as running, stair climbing, and descending[8]. However, accurately predicting plantar pressure distribution from IMU data remains a significant challenge. O'Reilly et al. pointed out that the main issues currently faced by IMU systems are sensor misalignment, bias, and white noise, which can affect the accuracy of the data. Additionally, issues such as sensor calibration and alignment still need to be addressed in order to reduce data errors[20]. Existing studies often employ statistical models or traditional machine learning approaches, but these methods demonstrate limitations in handling complex temporal data and capturing the non-linear relationships between segmental kinematics and plantar pressure distributions[18].

Convolutional Neural Networks (CNN) represent a promising approach for modeling the relationship between human movement and wearable sensor data. Chhoeum et al. successfully modeled the relationship between plantar pressure mapping images and knee joint angles, achieving knee joint angle estimation from plantar pressure images while wearing three different types of footwear[6]. Long Short-Term Memory (LSTM) networks are a specialized variant of recurrent neural networks (RNNs) designed to handle sequential data. In Xiang et al.'s research, they implemented LSTM networks for predicting ankle joint angles, torques, and contact forces using IMUs[34]. Similarly, Zhang et al. used LSTM to accurately predict joint moments for ankle, knee, and hip joints based on joint angles and EMG signals from multiple movements[39]. In contrast, this study introduces a novel hybrid deep learning model combining CNN, bidirectional LSTM (BiLSTM), and a temporal attention mechanism to predict dynamic plantar pressure distribution from IMU data~~., our approach achieves superior performance (MSE=0.98, SSIM=0.89).~~

The aim of this study is to develop an accurate, portable, and cost-effective method for predicting comprehensive plantar pressure distributions using wearable IMU technology. Specifically, the model aims to capture the plantar pressure distribution throughout dynamic movements, encompassing various regions of the foot, thereby facilitating real-time gait analysis and supporting applications in clinical diagnosis, rehabilitation, and performance enhancement. Through this research, we intend to provide novel technical solutions for

personalized rehabilitation, sports performance optimization, and the development of wearable devices.

2 Materials and Methods

2.1 Data Collection

2.1.1 Participants

A total of 25 healthy adults (13 males, 12 females; age: 23.50 ± 0.84 years; height: 174.20 ± 5.50 cm; weight: 73.3 ± 10.6 kg) participated in the experiment to collect data. The inclusion criteria for participants were as follows: 1) Participants had no history of lower limb surgery; 2) Participants had no injury-related factors that could interfere with the study in the past six months; 3) Participants were required to be free of any neurological disorders to ensure the internal validity of the study.; 4) Participants with a dominant right foot were aged between 18 and 45 years, exhibited a stable gait pattern, and had no noticeable limping or abnormal gait. All participants provided written informed consent for the experimental procedures, and the study was approved by the Ethics Committee of Ningbo University (TY2025033). This study strictly adhered to the principles outlined in the Declaration of Helsinki.

2.1.2 Experimental set-up and protocol

Before the experiment, each participant was required to be barefoot to ensure accurate plantar pressure measurements and eliminate the interference caused by different shoes[3],[40]. They were also equipped with the Xsens Suit Configuration (Movella Technologies, Enschede, Netherlands). This suit included eight Xsens inertial sensors, which were positioned according to the predefined sensor placements outlined in the Xsens Link manual[19]. The sensors were secured using Velcro straps and designated pockets integrated into the suit. The suit size was adjusted according to each participant's body shape to ensure a snug fit, maintaining consistent sensor positioning and minimizing measurement errors resulting from sensor displacement[23],[38](The IMU placement is detailed in the Supplementary Files Figure S2.).Since the participants were barefoot, they were instructed to walk freely for 10 minutes prior to the experiment to familiarize themselves with the setup and ensure that no discomfort was experienced due to overly tight sensor placement. To ensure the collected data accurately reflected a natural walking pattern, the first step of the experiment involved determining each participant's tailored preferred walking speed (T-PWS). This approach is crucial as walking at

a self-selected speed is known to minimize gait variability, leading to a more stable and representative movement pattern for analysis. To achieve this, the treadmill's digital speed display was obscured from view. Participants commenced walking at a slow speed, and the investigator gradually increased the speed in increments of 0.1 km/h until the participant reported that they had reached their optimal T-PWS. Subsequently, the speed was increased by 1.5 km/h and then gradually decreased in increments of 0.1 km/h to reestablish the T-PWS. This process was repeated three times, ensuring a variation of less than 0.4 km/h, and the average speed was computed to establish the final T-PWS[13]. Subsequently, calibration was conducted using the Zebris FDM system (Gait Analysis Model FDM-TDSL-3i, Zebris Inc.®, Germany) and Xsens MVN Analyze Pro software in accordance with the respective manuals to eliminate experimental errors. Upon achieving satisfactory calibration results, participants proceeded to walking on a treadmill embedded with the Zebris pressure plate at the previously determined T-PWS (with a 0° incline). Data collection commenced once a stable gait was achieved (approximately 1.5 minutes into the trial), as the coefficient of variation for stride length and stride time reaches its minimum under stable gait conditions[17]. Two software were then used simultaneously to record plantar pressure data and corresponding inertial sensor data for a duration of 30 seconds[36]. This procedure was repeated six times.

2.2 Data Preprocessing

2.2.1 Dealing with IMU Data

The IMU data were collected using Xsens MVN Analyze Pro (2024.2) software at a sampling frequency of 100 Hz in "On-Body Recording Mode". Each sensor captured motion across three anatomical planes (coronal, sagittal, and transverse) and six movement directions (as shown in Figure 1A). Post-processing of all motion measurements was conducted using the software's "High-Definition Reprocessing" mode and the "No-Level" processing scenario.

In this scenario, the pelvis segment was spatially fixed, and all kinematic variables were expressed relative to the pelvis, which is the recommended approach for joint angle analysis in biomechanics[25].

During this phase, the software computed the 3D joint angles for all joints within the Xsens biomechanical model, adhering to the ~~the~~ International Society of Biomechanics (ISB) guidelines for defining the coordinate systems of the ankle, knee, and hip joints[33].

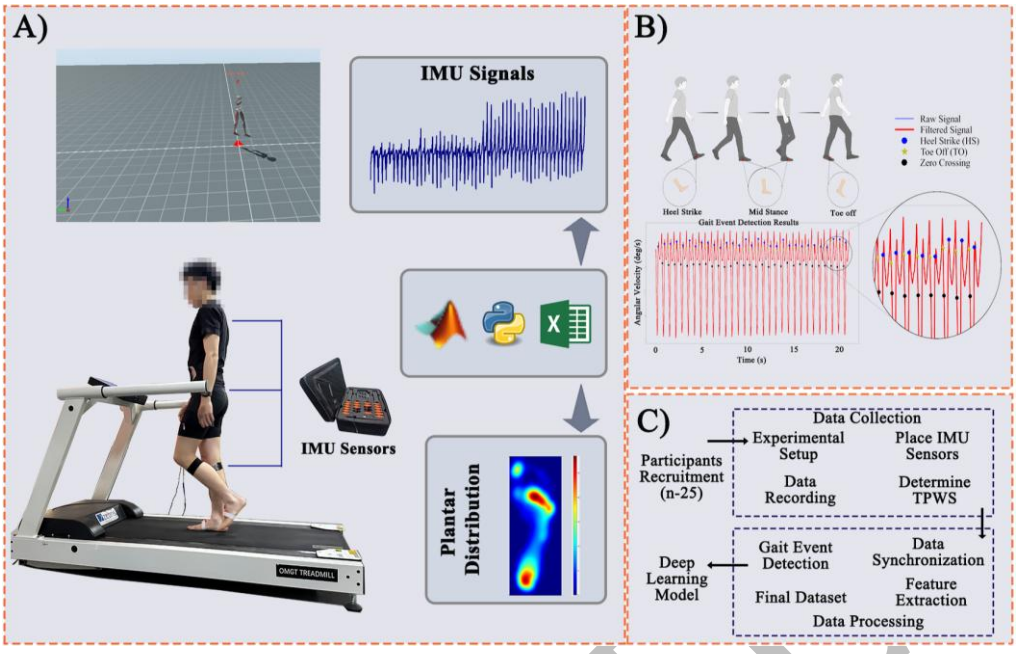

Figure 1 Overview of the Experimental and Data Analysis Workflow. A) Experimental protocol; B) Gait event detection; C) Experimental flow chart

We utilized the angular velocity data obtained from the processed lower-leg sensor to define gait events, specifically heel strike (HS) and toe-off (TO), which together constitute the stance phase of a single gait cycle. The gait angular velocity data collected by Xsens were processed using a third-order Butterworth low-pass filter. This filter was designed with a sampling frequency of 100 Hz and a cutoff frequency of 20 Hz to achieve zero-phase filtering, effectively eliminating phase delays and ensuring accurate signal processing[2]. For HS detection, after eliminating spurious noise using the 20 Hz low-pass zero-phase lag filter, an automated Python program was employed to reliably identified peaks in the gyroscope signal. These peaks, as supported by previous research, were precisely defined as HS points[2],[9]. However, for TO detection, we observed that the peak immediately following HS did not correspond precisely to the TO point. Instead, TO occurred with a noticeable delay relative to the subsequent peak after HS. According to the zero-crossing detection method proposed by Bötzel et al.[2], the TO point was defined as:

$$TO_{position} = \text{peak height} + 0.49 \times (\text{zero-crossing position} - \text{peak position}) \quad (1)$$

where the zero-crossing point was defined as the point where the signal transitioned from positive to negative after the initially assumed TO peak. The coefficient 0.49 was the optimal value for comprehensive multi-speed scenarios. The TO point defined under this coefficient

was closest to the TO point measured by the pressure insole, with a standard deviation of 0.16. Following the above methodology, the gait events in Xsens data were accurately identified and extracted with high precision by a custom Python program. The detailed gait event definition process is clearly illustrated in Figure 1B, and the whole experimental process is illustrated in Figure 1C.

2.2.2 Plantar pressure

While wearing Xsens inertial sensors, participants walked on a treadmill embedded with a pressure mat at a 0% incline and at their PWS. The Zebris system recorded plantar pressure distribution at a sampling frequency of 120 Hz.

Raw XML files were exported using the Zebris FDM software, containing detailed pressure values (unit: N/cm²) collected by each pressure sensor during each stance phase. A custom Python script was used to extract and save the detailed pressure values of every frame for each stance phase as CSV files, with each file labeled according to its corresponding gait cycle number.

Finally, the IMU data obtained from the Xsens sensors and the plantar pressure data were synchronized using a Python script. Cubic spline interpolation was applied to the Xsens data, and they were aligned with the gait events, representing 0% to 100% of a complete stance phase. To ensure dataset accuracy and completeness, trials with abnormal values or missing data were automatically excluded from the analysis.

The experiment was repeated six times, resulting in a total collection of 1,808 entries of IMU data and 1,825 entries of plantar pressure data. After preprocessing, which involved removing unsynchronized data and data with obvious outliers, 1,737 matched pairs of Xsens data and plantar pressure data were retained as the dataset for training the model.

2.3 Building a Hybrid CNN-BiLSTM Architecture

This study innovatively employs a CNN-BiLSTM-Attention deep learning model. The motivation for this architecture is to leverage the distinct strengths of each component for gait data analysis. We use a CNN to automatically extract local, transient features from the raw IMU time-series data, such as the rapid changes during heel strike. Subsequently, a BiLSTM network is employed to model the long-range temporal dependencies inherent in a full gait cycle, capturing the entire sequence from start to finish. Finally, a temporal attention mechanism is

integrated to allow the model to dynamically weigh the importance of different time steps, focusing on the most biomechanically significant moments for pressure prediction.

As a supervised learning approach, CNN-BiLSTM-Attention is capable of capturing the temporal dependencies between input and output data[21],[37]. This approach is used to predict the plantar pressure distribution based on the corresponding lower-limb kinematic parameters at each time step. The detailed workflow of the model, from input to output, is illustrated in Figure 2D. The input data first passes through a single-layer 1D-CNN (kernel size of 3, 256 filters) to extract 256 feature channels from 18 input channels (Figure 2A), followed by the Rectified Linear Unit (ReLU) activation and BatchNorm1D to enhance stability[11]. Subsequently, the features are fed into a three-layer BiLSTM (Figure 2C) to capture long-term dependencies in the time series (a detailed architecture of a single LSTM unit is depicted in Figure 2B). Next, a temporal attention mechanism (Figure 2E) weights the LSTM outputs, focusing on critical time steps to generate a weighted context vector[31]. Finally, the body weight feature is transformed into a higher-dimensional representation via fully connected layers, concatenated with the weighted features, and passed through a decoder to produce personalized plantar pressure predictions. Figure 2D presents the complete architecture of the CNN-BiLSTM-Attention model. More details are provided in the supplementary file.

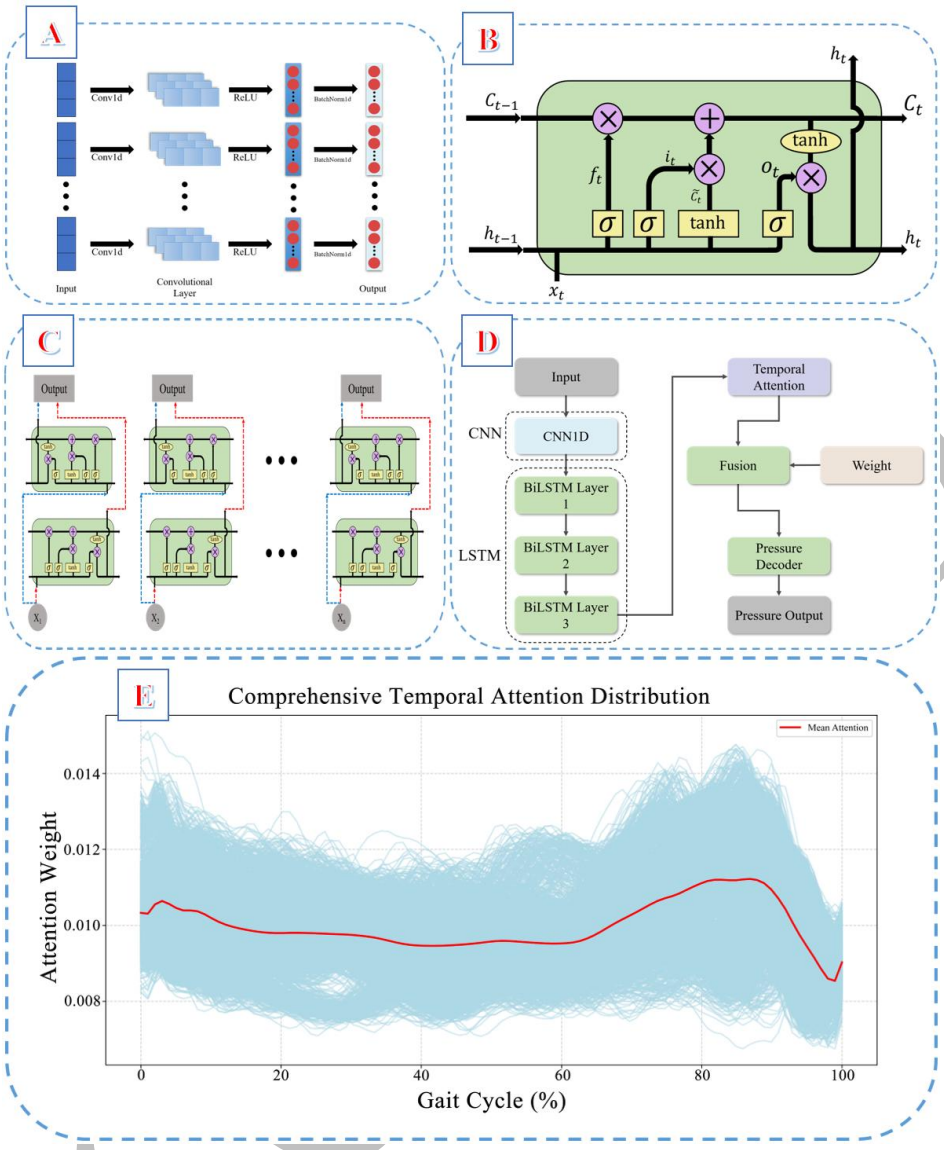

Figure 2 The specific architecture, workflow, and attention mechanism of the model

2.4 Hyperparameters

Hyperparameters for the CNN and BiLSTM modules were optimized using the Optuna framework[1]. The attention mechanism was not a primary focus for tuning, as its parameters are relatively few, and preliminary experiments indicated that classic configurations adequately captured temporal features[31]. The final hyperparameter configuration, selected based on achieving the lowest validation loss, is presented in Table 1. A detailed account of the specific tuning procedures is provided in the Supplementary File (Text S2).

Table1. Optimal parameter configuration of the CNN-BiLSTM-Attention model

Parameter	Configuration
Batch Size	32

Epochs	35
Dropout Rate	0.17
Learning Rate	1.86e-4
Optimizer	Adam

2.5 Training

We divided the entire dataset in a 7:3 ratio into a training set (70%) and a test set (30%), ensuring the test set remained completely independent from the model training and validation process. On the training set, we employed 10-fold cross-validation to evaluate the model. The process involved dividing the training set into 10 non-overlapping subsets, using 9 subsets to train the model during each iteration while the remaining subset served as the validation set, this process was repeated 10 times, ensuring that each subset served as the validation set exactly once[15]. Through this 10-fold cross-validation approach, we derived a final model. Finally, we evaluated the performance of this final model on the previously unseen test set. The primary goal of the training is to enable the model to accurately predict the distribution of plantar pressure. During training, we use MSE as the cost function, which minimizes the squared error between the predicted pressure map and the ground truth pressure map to adjust the model's parameters and improve prediction accuracy.

$$\mathrm{MSE} = \frac{1}{N}\sum_{i=1}^{N}(y_i - \hat{y}_i)^2 \tag{2}$$

Where N represents the number of samples, y_i represents the true pressure value for the i-th sample, and $\hat{y}_i$ represents the predicted pressure value for the i-th sample. The MSE is computed based on the error of each pressure point, rather than simply summing all pressure values.

In addition, we use several other evaluation metrics to assess the model's performance, including Mean Absolute Error (MAE), Root Mean Squared Error (RMSE), Coefficient of Determination (R^2 Score), Structural Similarity Index (SSIM), and Peak Pressure Error (PPE):

$$\mathrm{MAE} = \frac{1}{N}\sum_{i=1}^{N}|y_i - \hat{y}_i| \tag{3}$$

MAE Calculates the absolute error between predicted and true values, giving a straightforward measure of the average prediction error (in units of N/cm^2).

$$\text{RMSE} = \sqrt{\frac{1}{N}\sum_{i=1}^{N}(y_i - \hat{y}_i)^2} \tag{4}$$

RMSE emphasizes larger errors more than MAE, making it more sensitive to larger deviations (in units of N/cm²).

$$R^2 = 1 - \frac{\sum_{i=1}^{N}(y_i - \hat{y}_i)^2}{\sum_{i=1}^{N}(y_i - \bar{y})^2} \tag{5}$$

R^2: Reflects the goodness of fit of the model. An R^2 value closer to 1 indicates better model fit.

$$\text{SSIM}(x, y) = \frac{(2\mu_x\mu_y + C_1)(2\sigma_{xy} + C_2)}{(\mu_x^2 + \mu_y^2 + C_1)(\sigma_x^2 + \sigma_y^2 + C_2)} \tag{6}$$

SSIM measures the structural, brightness, and contrast similarity between the predicted and true pressure maps. It ranges from 0 to 1, where a value closer to 1 indicates a more accurate prediction of plantar pressure distribution. μ_x and μ_y represent the mean pixel values of images x and y, respectively. σ_x^2 and σ_y^2 are the variances of images x and y, and σ_{xy} is the covariance between x and y[32].

$$\text{PPE} = |\max(y) - \max(\hat{y})| \tag{7}$$

PPE measures the error between the predicted and true maximum pressure values, assessing the model's ability to predict high-pressure areas (in units of N/cm²).

To reduce overfitting in the neural network, we employ the ReduceLROnPlateau learning rate scheduler and the best model saving mechanism as part of the early stopping strategy. Specifically, we use ReduceLROnPlateau to monitor the validation loss[27]. If the validation loss does not decrease after 5 consecutive training rounds, the learning rate is automatically reduced by 50% to prevent the model from getting stuck in local optima or experiencing vanishing gradients. Additionally, after each epoch, we check the current model's validation loss and save the model with the lowest validation loss, ensuring that the model with the best generalization ability is used for final evaluation. Since the learning rate continuously decreases, the update step size for model parameters becomes smaller as the model converges, stabilizing the training process and leading to natural termination. This strategy effectively reduces unnecessary training cycles, improves training efficiency, and ensures the optimal performance

of the final model.

3 Results

Figure 3A illustrates the angular velocity profiles of the right lower limb segments—including the thigh, shank, and foot. These profiles are presented along all three anatomical axes (X, Y, and Z). Figure 3B displays the corresponding joint angle trajectories of the right hip, knee, and ankle, providing a detailed depiction of lower limb articulation throughout the stance phase.

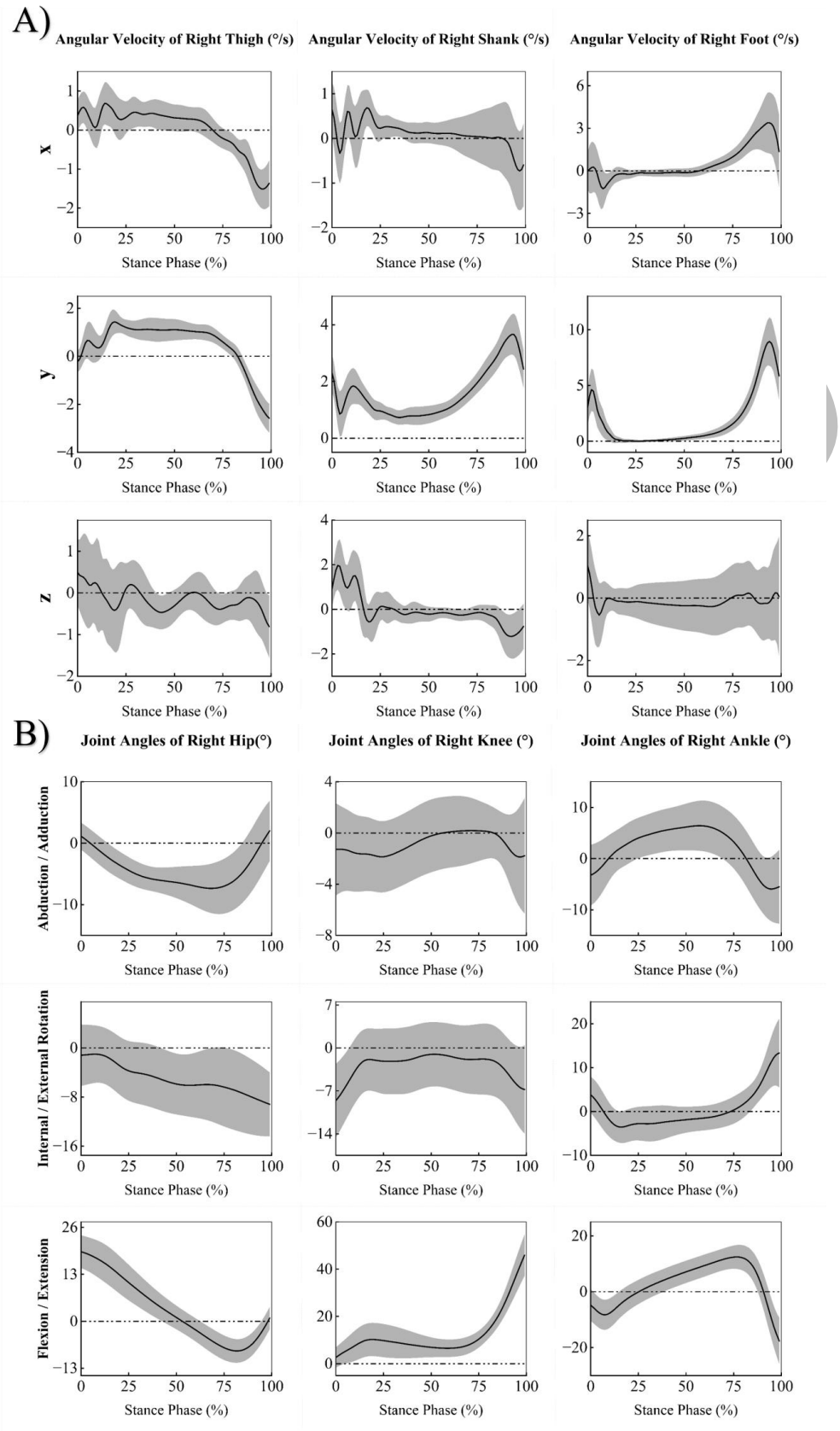

Figure 3 Features of IMU data. Figure A presents the angular velocity data of the lower limb joints. The first column shows the angular velocities of the right thigh in the X, Y, and Z axes,

the second column corresponds to the right shank angular velocities in the X, Y, and Z axes, and the third column represents the right foot angular velocities in the X, Y, and Z axes. Figure B presents the joint angle data of the lower limbs. The first column shows the right hip joint movements in adduction/abduction, internal/external rotation, and flexion/extension. The second column shows the knee joint movements in adduction/abduction, internal/external rotation, and flexion/extension. The third column shows the ankle joint movements in inversion/eversion, internal/external rotation, and plantarflexion/dorsiflexion. The black line in the figure represents the mean, while the light black area indicates the standard deviation.

Table2. The mean value and standard deviation of MAE, RMSE, R^2, SSIM and PPE

Metric	Mean±SD
MAE	0.2971±0.0101
RMSE	0.9332±0.0314
R^2	0.8943±0.0169
SSIM	0.8911±0.0051
PPE	4.0210±0.3476

As shown in the Table 2 and Figure 4 the proposed CNN-LSTM-Attention model performs excellently across all evaluation metrics. The low MAE of 0.2971 N/cm² and RMSE of 0.9332 N/cm² indicate a small average prediction error between the predicted and actual pressure values. The high R^2 of 0.8943 signifies that the model can explain a large portion of the variance in the plantar pressure data, indicating a strong goodness of fit. Furthermore, the SSIM of 0.8911 is particularly noteworthy, as it confirms that the predicted pressure maps have a high degree of structural resemblance to the actual maps, which is crucial for biomechanical analysis. Finally, the PPE of 4.0210 N/cm² shows the model's proficiency in predicting the high-pressure regions, which are often of clinical significance.

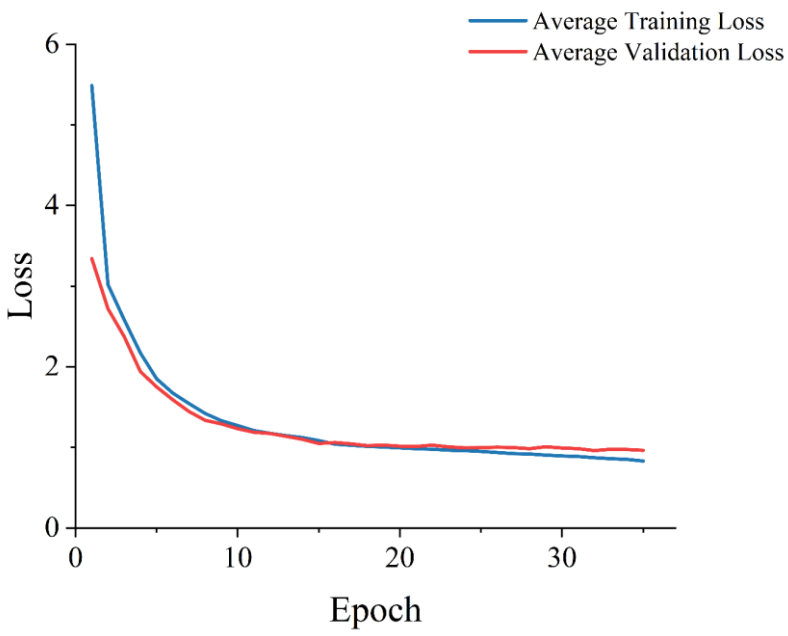

Figure 4 10-Fold Cross-Validation Average Loss Curve. The plot displays the mean loss value at each training epoch. The close convergence of the training and validation loss curves indicates that the model learned effectively without significant overfitting.

The prediction visualizations (Figure 5) further demonstrate the model's high performance. The predicted pressure map is very close to the actual pressure distribution. This indicates that the model is capable of accurately predicting the pressure distribution and values during walking, while also effectively capturing high-pressure regions and the overall load pattern.

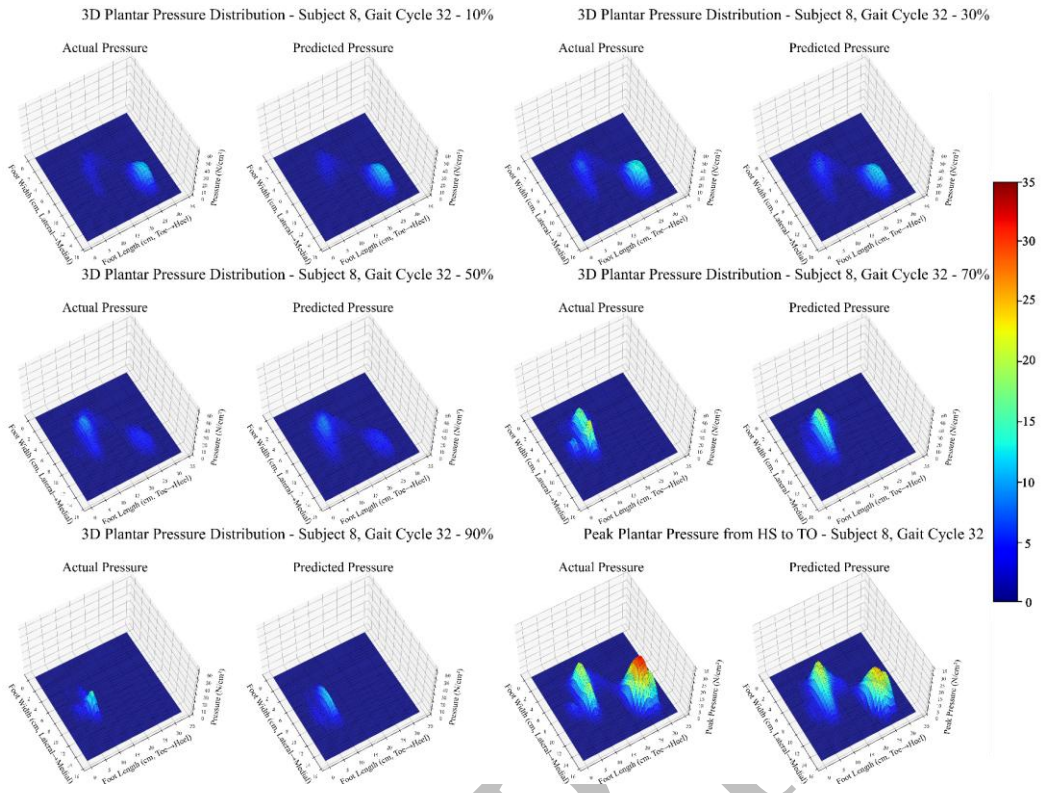

Figure 5 3D visualization of actual pressure and predicted pressure. There are 6 pairs of images in total. The first five pairs of images show the actual plantar pressure images and predicted plantar pressure at 10%, 30%, 50%, 70% and 90% of the stance phase respectively. The last pair of images shows the actual image and predicted image of the peak plantar pressure recorded during the entire stance phase.

Further analysis of the two-dimensional heat maps (Figure 6) confirms that the model intuitively captures the dynamic distribution pattern of plantar pressure. Despite this strong overall performance, these visualizations also reveal local prediction errors in the pressure distribution. For instance, although the SSIM value reached approximately 0.89, deviations were frequently noted between the predicted and actual pressure values, particularly in the medial arch region, suggesting that the model may struggle to accurately capture pressure characteristics in this specific area. Moreover, discrepancies between the predicted and actual pressure magnitudes were also identified; the PPE value reached around 4, corresponding to 4 N/cm^2, indicating that the model was unable to predict the absolute pressure values in certain regions with high accuracy.

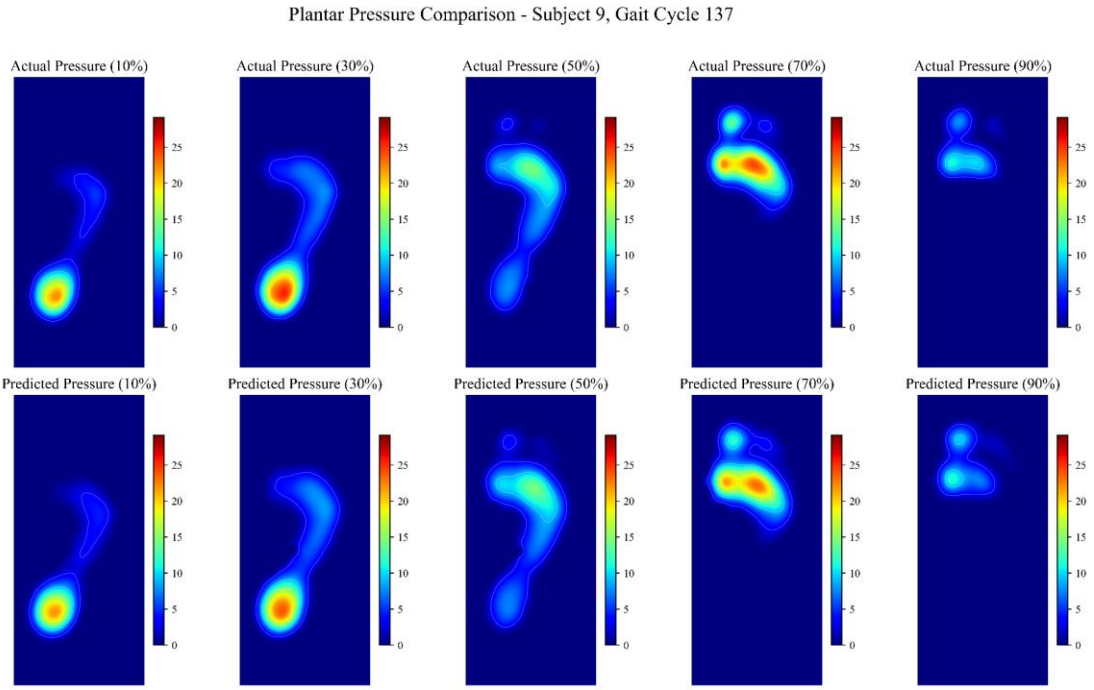

Figure 6 2D visualization of actual pressure and predicted pressure. The image contains five pairs of figures. The top five images represent the actual plantar pressure distributions at 10%, 30%, 50%, 70%, and 90% of the stance phase, respectively. The bottom five images show the corresponding predicted plantar pressure distributions at 10%, 30%, 50%, 70%, and 90% of the stance phase.

4 Discussion

This study aims to estimate the corresponding plantar pressure distribution and values using a CNN-LSTM-Attention hybrid deep learning model, based on lower limb kinematic data recorded by IMUs. The model leverages CNN's ability to extract local features from time-series data recorded by IMUs, capturing dynamic changes throughout the gait cycle. Additionally, LSTM models the temporal dependencies in the data through its recursive structure, capturing how data evolves over time. The attention mechanism weights the importance of different time steps, allowing the model to focus on time steps that are more important for prediction. This combination effectively aligns with the biomechanical patterns in the gait cycle, specifically the process from HS to TO. The prediction results (MAE=0.297, RMSE=0.933, R^2=0.894, SSIM=0.891) indicate that the model accurately captures the primary characteristics of plantar pressure distribution during the stance phase.

The model's accuracy in predicting plantar pressure distribution is primarily attributed to

its design, including the synergistic interaction between CNN, BiLSTM networks, and the temporal attention mechanism[35]. Specifically, the CNN layer extracts local features from the IMUs data, such as variations in joint angular velocity or transient patterns in joint angles. After convolution, the input data are transformed into high-dimensional features that capture local temporal dynamics within the gait cycle, such as the instantaneous movement characteristics during foot swing or ground contact. The low RMSE in the experimental results suggests that the CNN effectively extracts key motion information related to plantar pressure, laying the foundation for subsequent time series modeling. The BiLSTM layer further processes the feature sequences extracted by CNN. The memory capability of the BiLSTM enables it to capture long-term dependencies in the gait cycle, such as the pressure transfer process from HS to TO. The bidirectional design enables the model to simultaneously incorporate information from both past and future time steps, thereby ensuring a comprehensive understanding of the dynamic changes occurring throughout the gait cycle[26]. The high R^2 value indicates that the BiLSTM successfully explains the trend of pressure distribution changes over time, which is crucial for predicting continuous plantar pressure distributions.

Traditional models often treat all time steps equally, making it difficult to highlight key moments in the gait cycle. The introduction of an additional temporal attention mechanism allows the model to focus on more important time steps within the gait cycle, bringing a unique biomechanical perspective to the model. Specifically, in the gait cycle, certain time steps, such as peak pressure moments, have a much greater impact on the results than others. The adaptive weight adjustment capability of the attention mechanism allows the model to invest more "attention" at these key points, thereby reducing prediction errors. From the visualization of the temporal attention mechanism, we found that the model allocated higher attention values at critical moments in the gait cycle, such as HS and TO moments. This highly aligns with the biomechanics of plantar pressure changes, as peak plantar pressure in the hindfoot occurs during HS while peak pressure in the forefoot occurs during TO. This perspective suggests that the model not only achieves high prediction accuracy but also demonstrates an understanding of the biomechanical relationship between lower limb kinematics and plantar pressure, thereby enhancing its explainability.

In previous research, few researchers have predicted plantar pressure through lower limb

kinematic data. In the study by Animesh Hazari et al., a clinically applicable regression model was developed for diabetic patients using multivariate linear regression to predict peak plantar pressure during walking, aiding in ulcer risk assessment, achieving an R^2 of 0.908[10]. However, this was limited to peak plantar pressure, and multivariate linear regression cannot capture the dynamic characteristics of time-series data. Raquel Sánchez Rodríguez et al. investigated the relationship between foot posture and plantar pressure patterns during gait, also using multivariate linear regression to explore whether the Foot Posture Index (FPI) or its individual criteria could predict dynamic plantar pressure in different regions. Their results showed that while certain calcaneal frontal plane positions and talonavicular joint prominence had some influence on plantar pressure prediction, the ability to predict plantar pressure using this method was relatively limited(R^2=0.111)[24]. This indicates that FPI has weak predictive power, especially in the forefoot region, with predictive effects mainly concentrated on hindfoot and midfoot pressure. Su-Bin Joo et al. used pressure insoles to record plantar pressure and an ANN model to predict corresponding gait cycle speed based on plantar pressure. By inputting plantar pressure data from both stance and swing phases, they predicted speed throughout the entire gait cycle with relatively high accuracy (R^2=0.730)[12]. In contrast, our research focuses on predicting plantar pressure based on lower limb kinematic data. While our prediction target differs from previous studies, all revolve around plantar pressure. This paper employed various metrics to measure the model's overall performance (MSE, MAE, RMSE, R^2, SSIM). The SSIM was innovatively introduced to evaluate the spatial structural similarity between predicted and actual plantar pressure maps. This is particularly important in biomechanics, as the spatial relationship of plantar pressure distribution serves as a crucial indicator in clinical diagnosis. The high SSIM value also demonstrates the model's efficient performance from a biomechanical perspective. Additionally, during 10-fold cross-validation, we found minimal differences between different folds, further indicating our model's high generalization capability.

Nevertheless, our research has certain limitations. First, the dataset is limited by its small size (N=25) and demographic homogeneity, as the cohort consists exclusively of healthy young adults. This restricts the model's current generalizability to other populations, such as older adults. Second, the analysis was restricted to the dominant right limb to ensure consistency,

which limits the findings' applicability to bilateral assessments or individuals with gait asymmetries. Third, the model lacks anatomical foot constraints such as foot width or arch index, which may contribute to prediction inaccuracies in specific regions like the medial arch. Future research could address this by incorporating multi-segment foot models.

5 Conclusion

This study proposes an innovative, cost-effective, and portable approach for predicting plantar pressure distribution using IMU data. We developed a sophisticated deep learning framework that integrates CNN, BiLSTM networks, and a temporal attention mechanism, effectively capturing the complex spatiotemporal relationships between lower limb kinematics and plantar pressure. The final model achieved an RMSE of 0.93, an R^2 of 0.89, an SSIM of 0.89, and a PPE of 4.02, demonstrating its high prediction accuracy.

Acknowledgments: The author wishes to thank all the authors and participants who actively participated in this study.

Funding statement : This study was sponsored by National Key R&D Program of China (2024YFC3607305), Zhejiang Province Science Fund for Distinguished Young Scholars (LR22A020002), Zhejiang Provincial Key Project of Education Science Planning (2025SB084), Zhejiang Engineering Research Center for New Technologies and Applications of Helium-Free Magnetic Resonance Imaging Open Fund Project 2024 (2024GCPY02), Ningbo Key Research and Development Program (Grant number: 2022Z196), Zhejiang Rehabilitation Medical Association Scientific Research Special Fund (ZKKY2023001), Research Academy of Medicine Combining Sports, Ningbo (No.2023001), Ningbo Clinical Research Center for Orthopedics and Exercise Rehabilitation (No.2024L004), Ningbo Natural Science Foundation (Grant number: 2022J065) and K. C. Wong Magna Fund in Ningbo University.

Reference

[1] Akiba T., Sano S., Yanase T., Ohta T., Koyama M., Optuna: A next-generation hyperparameter optimization framework, in: Proceedings of the 25th ACM SIGKDD International Conference on Knowledge Discovery & Data Mining, ACM, Anchorage AK USA, 2019:2623-2631. DOI: 10.1145/3292500.3330701.

[2] Bötzel K., Marti F.M., Rodríguez M.Á.C., Plate A., Vicente A.O., Gait recording with inertial sensors – how to determine initial and terminal contact, J Biomech, 2016, 49(1):332–337. DOI: 10.1016/j.jbiomech.2015.12.035.

[3] Cen X., Song Y., Yu P., Sun D., Simon J., Bíró I., Gu Y., Effects of plantar fascia stiffness on the internal mechanics of idiopathic pes cavus by finite element analysis: Implications for metatarsalgia, Comput Methods Biomech Biomed Eng, 2024, 27(14):1961-1969. DOI: 10.1080/10255842.2023.2292723.

[4] Cen X., Yu P., Song Y., Sun D., Liang M., Bíró I., Gu Y., Influence of medial longitudinal arch flexibility on lower limb joint coupling coordination and gait impulse, Gait Posture, 2024, 114:208–214. DOI: 10.1016/j.gaitpost.2024.05.011.

[5] Chehab E.F., Andriacchi T.P., Favre J., Speed, age, sex, and body mass index provide a rigorous basis for comparing the kinematic and kinetic profiles of the lower extremity during walking, J Biomech, 2017, 58:11–20. DOI: 10.1016/j.jbiomech.2017.04.014.

[6] Chhoeum V., Kim Y., Min S.D., A convolution neural network approach to access knee joint angle using foot pressure mapping images: a preliminary investigation, IEEE Sensors J, 2021, 21(15):16937–16944. DOI: 10.1109/JSEN.2021.3079516.

[7] Gao S., Song Y., Sun D., Cen X., Wang M., Lu Z., Gu Y., Impact of Becker muscular dystrophy on gait patterns: Insights from biomechanical analysis, Gait Posture, 2025. (Note: As this is a future publication, volume, page, and DOI information may not yet be available).

[8] Hamdi M.M., Awad M.I., Abdelhameed M.M., Tolbah F.A., Lower limb motion tracking using IMU sensor network, in: 2014 Cairo International Biomedical Engineering Conference (CIBEC), 2014:28-33. DOI: 10.1109/CIBEC.2014.7020957.

[9] Hannink J., Kautz T., Pasluosta C.F., Gaßmann K.-G., Klucken J., Eskofier B.M., Sensor-based gait parameter extraction with deep convolutional neural networks, IEEE J Biomed Health Inform, 2017, 21(1):85–93. DOI: 10.1109/JBHI.2016.2636456.

[10] Hazari A., Maiya A., Agouris I., Monteiro A., Shivashankara, Prediction of peak plantar pressure for diabetic foot: the regressional model, Foot, 2019, 40:87–91. DOI: 10.1016/j.foot.2019.06.001.

[11] Ioffe S., Szegedy C., Batch normalization: accelerating deep network training by reducing

internal covariate shift, in: Proceedings of the 32nd International Conference on Machine Learning, PMLR, 2015:448-456. http://proceedings.mlr.press/v37/ioffe15.html. Accessed April 11, 2025.

[12] Joo S.-B., Oh S.E., Sim T., Kim H., Choi C.H., Koo H., Mun J.H., Prediction of gait speed from plantar pressure using artificial neural networks, Expert Syst Appl, 2014, 41(16):7398–7405. DOI: 10.1016/j.eswa.2014.06.002.

[13] Jordan K., Challis J.H., Newell K.M., Walking speed influences on gait cycle variability, Gait Posture, 2007, 26(1):128–134. DOI: 10.1016/j.gaitpost.2006.08.010.

[14] Khuyagbaatar B., Tumurbaatar M., Tsenkherjav K., Purevsuren T., Shambaljamts T., Kim K., Kim Y.H., Kinematic comparison of snatch and clean lifts in weightlifters using wearable inertial measurement unit sensors, Phys Act Health, 2024, 8(1). DOI: 10.56286/pah.v8i1.309.

[15] Kohavi R., A study of cross-validation and bootstrap for accuracy estimation and model selection, in: Proceedings of the 14th International Joint Conference on Artificial Intelligence (IJCAI), 1995, 2:1137–1143.

[16] Majumder S., Deen M.J., Wearable IMU-based system for real-time monitoring of lower-limb joints, IEEE Sensors J, 2021, 21(6):8267–8275. DOI: 10.1109/JSEN.2020.3044800.

[17] Meyer C., Killeen T., Easthope C.S., Curt A., Bolliger M., Linnebank M., Zörner B., Filli L., Familiarization with treadmill walking: how much is enough?, Sci Rep, 2019, 9:5232. DOI: 10.1038/s41598-019-41721-0.

[18] Moon J., Lee D., Jung H., Choi A., Mun J.H., Machine learning strategies for low-cost insole-based prediction of center of gravity during gait in healthy males, Sensors (Basel), 2022, 22(9):3499. DOI: 10.3390/s22093499.

[19] Myn U., Link M., Awinda M., Xsens Mvn User Manual, Xsens Motion Technol. BV, Enschede Neth, 2015.

[20] O'Reilly M., Caulfield B., Ward T., Johnston W., Doherty C., Wearable inertial sensor systems for lower limb exercise detection and evaluation: a systematic review, Sports Med, 2018, 48(5):1221–1246. DOI: 10.1007/s40279-018-0878-4.

[21] Ordóñez F.J., Roggen D., Deep convolutional and LSTM recurrent neural networks for multimodal wearable activity recognition, Sensors, 2016, 16(1):115. DOI:

10.3390/s16010115.

[22] Raza A., Mahmood I., Sultana T., Evaluation of weight-bearing, walking stability, and gait symmetry in patients undergoing restoration following hip joint fractures, Int J Biomed Eng Technol, 2025, 47(3):195-213. DOI: 10.1504/IJBET.2025.144815.

[23] Roetenberg D., Luinge H., Slycke P., Xsens MVN: Full 6DOF Human Motion Tracking Using Miniature Inertial Sensors, Xsens Technologies B.V., 2009.

[24] Sánchez-Rodríguez R., Martínez-Nova A., Escamilla-Martínez E., Pedrera-Zamorano J.D., Can the foot posture index or their individual criteria predict dynamic plantar pressures?, Gait Posture, 2012, 36(4):591–595. DOI: 10.1016/j.gaitpost.2012.05.024.

[25] Schepers M., Giuberti M., Bellusci G., Xsens MVN: Consistent tracking of human motion using inertial sensing, Xsens Technologies, 2018. DOI: 10.13140/RG.2.2.22099.07205.

[26] Siami-Namini S., Tavakoli N., Namin A.S., The performance of LSTM and BiLSTM in forecasting time series, in: 2019 IEEE International Conference on Big Data (Big Data), 2019:3285-3292. DOI: 10.1109/BigData47090.2019.9005997.

[27] Smith L.N., Cyclical learning rates for training neural networks, in: 2017 IEEE Winter Conference on Applications of Computer Vision (WACV), 2017:464-472. DOI: 10.1109/WACV.2017.58.

[28] Song Y., Cen X., Sun D., Bálint K., Wang Y., Chen H., Gu Y., Curved carbon-plated shoe may further reduce forefoot loads compared to flat plate during running, Sci Rep, 2024, 14(1):13215. DOI: 10.1038/s41598-024-63385-z.

[29] Song Y., Cen X., Wang M., Bálint K., Tan Q., Sun D., Zhang M., The influence of simulated worn shoe and foot inversion on heel internal biomechanics during running impact: A subject-specific finite element analysis, J Biomech, 2025, 180:112517. DOI: 10.1016/j.jbiomech.2024.112517.

[30] Song Y., Cen X., Wang M., Gao Z., Tan Q., Sun D., Zhang M., A Systematic Review of Finite Element Analysis in Running Footwear Biomechanics: Insights for Running-Related Musculoskeletal Injuries, J Sports Sci Med, 2025, 24(2):370. (Note: Please verify if a DOI is available closer to the publication date).

[31] Vaswani A., Shazeer N., Parmar J., Uszkoreit J., Jones L., Gomez A.N., Kaiser Ł., Polosukhin I., Attention is all you need, in: Advances in Neural Information Processing

Systems 30 (NIPS 2017), Curran Associates, Inc., 2017:5998-6008. https://proceedings.neurips.cc/paper_files/paper/2017/hash/3f5ee243547dee91fbd053c1c4a845aa-Abstract.html. Accessed March 20, 2025.

[32] Wang Z., Bovik A.C., Sheikh H.R., Simoncelli E.P., Image quality assessment: From error visibility to structural similarity, IEEE Trans Image Process, 2004, 13(4):600–612. DOI: 10.1109/TIP.2003.819861.

[33] Wu G., Siegler S., Allard P., Kirtley C., Leardini A., Rosenbaum M., Whittle M., D'Lima D.D., Cristofolini L., Witte H., Schmid O., Stokes I., Standardization and Terminology Committee of the International Society of Biomechanics, ISB recommendation on definitions of joint coordinate system of various joints for the reporting of human joint motion--part I: Ankle, hip, and spine, J Biomech, 2002, 35(4):543–548. DOI: 10.1016/s0021-9290(01)00222-6.

[34] Xiang L., Gu Y., Gao Z., Yu P., Shim V., Wang A., Fernandez J., Integrating an LSTM framework for predicting ankle joint biomechanics during gait using inertial sensors, Comput Biol Med, 2024, 170:108016. DOI: 10.1016/j.compbiomed.2024.108016.

[35] Xiao Y., Yin H., Zhang Y., Qi H., Zhang Y., Liu Z., A dual-stage attention-based conv-LSTM network for spatio-temporal correlation and multivariate time series prediction, Int J Intell Syst, 2021, 36(5):2036–2057. DOI: 10.1002/int.22370.

[36] Yang F., King G.A., Dynamic gait stability of treadmill versus overground walking in young adults, J Electromyogr Kinesiol, 2016, 31:81–87. DOI: 10.1016/j.jelekin.2016.09.004.

[37] Zhan H., Kou J., Cao Y., Guo Q., Zhang J., Shi Y., Human gait phases recognition based on multi-source data fusion and BILSTM attention neural network, Measurement, 2024, 238:115396. DOI: 10.1016/j.measurement.2024.115396.

[38] Zhang J.-T., Novak A.C., Brouwer B., Li Q., Concurrent validation of xsens MVN measurement of lower limb joint angular kinematics, Physiol Meas, 2013, 34(8):N63–N71. DOI: 10.1088/0967-3334/34/8/N63.

[39] Zhang L., Soselia D., Wang R., Gutierrez-Farewik E.M., Lower-limb joint torque prediction using LSTM neural networks and transfer learning, IEEE Trans Neural Syst Rehabil Eng, 2022, 30:600–609. DOI: 10.1109/TNSRE.2022.3156786.

[40] Zhu C., Song Y., Xu Y., Zhu A., Baker J.S., Liu W., Gu Y., Toe box shape of running shoes affects in-shoe foot displacement and deformation: a randomized crossover study, Bioengineering, 2024, 11(5):457. DOI: 10.3390/bioengineering11050457.